



HAL
open science

Quantum size effects in Ag thin films grown on the fivefold surface of the icosahedral Al-Cu-Fe quasicrystal: Influence of the growth temperature

Ankit Shukla, Julian Ledieu, Émilie Gaudry, Dongmei Wu, Thomas Lograsso, Vincent Fournée

► **To cite this version:**

Ankit Shukla, Julian Ledieu, Émilie Gaudry, Dongmei Wu, Thomas Lograsso, et al.. Quantum size effects in Ag thin films grown on the fivefold surface of the icosahedral Al-Cu-Fe quasicrystal: Influence of the growth temperature. *Journal of Vacuum Science & Technology A*, 2022, 40 (1), pp.013212. 10.1116/6.0001450 . hal-03542010

HAL Id: hal-03542010

<https://hal.science/hal-03542010>

Submitted on 11 Oct 2022

HAL is a multi-disciplinary open access archive for the deposit and dissemination of scientific research documents, whether they are published or not. The documents may come from teaching and research institutions in France or abroad, or from public or private research centers.

L'archive ouverte pluridisciplinaire **HAL**, est destinée au dépôt et à la diffusion de documents scientifiques de niveau recherche, publiés ou non, émanant des établissements d'enseignement et de recherche français ou étrangers, des laboratoires publics ou privés.

Quantum size effects in Ag thin films grown on the 5-fold surface of the icosahedral Al-Cu-Fe quasicrystal: influence of the growth temperature.

A. K. Shukla,^{†,‡} J. Ledieu,[†] E. Gaudry,[†] D. M. Wu,[¶] T. A. Lograsso,[¶] and V.
Fournée^{*,†}

[†]*Institut Jean Lamour, UMR7198 CNRS-Nancy-Université de Lorraine, Campus ARTEM - 2 allée
André Guinier, BP 50840, 54011 Nancy, France*

[‡]*CSIR-National Physical Laboratory, DR. K. S. Krishnan Marg, New Delhi - 110012, India*

[¶]*Ames Laboratory, Division of Materials Sciences and Engineering, Ames, IA 50011, USA.*

E-mail: vincent.fournee@univ-lorraine.fr

Abstract

We have studied the growth and electronic structure of Ag thin films on the 5-fold surface of the icosahedral (*i*)-Al-Cu-Fe quasicrystal using scanning tunneling microscopy (STM), low energy electron diffraction (LEED), ultra-violet photoemission spectroscopy (UPS) and density functional theory (DFT). Upon deposition at 400 K, Ag islands grow to form crystallites with a preferred thickness for a given coverage. LEED patterns reveal five rotational domains of Ag crystallites with (111) orientation for coverages larger than ~ 7 monolayers. Quantum well states (QWS) are observed in the photoemission spectra of Ag/*i*-Al-Cu-Fe ranging from 5 to 35 monolayers, indicating electron confinement within the film thickness and thus

confirming electronic growth of Ag thin films on quasicrystalline surfaces. Electronic structure calculations have been performed to discuss the possible origins of the confinement at the film-substrate interface.

This article is dedicated to the memory of Pat Thiel who has been a leading scientist in the field of quasicrystal research and an inspirational guide for many of us.

Introduction

Nanoscale metallic structures have attracted immense interest due to their novel physical properties which are often different from the corresponding bulk metals. Thin metal films deposited on clean surfaces are examples of nanoscale structures. When the film thickness is smaller than the electron coherence length scale (nanoscale), electrons will preserve their phase information and can therefore no longer be regarded as a continuum or sea of electrons. This may lead to the creation of standing electron waves, or quantum well states (QWS) in thin films due to the confinement of electrons within the film thickness. It has been predicted that the electron density, Fermi energy, work function, charge spilling, and interlayer relaxation oscillate as a function of film thickness.¹⁻³ Since most of the materials properties directly depend on the density of states (DOS) and electron distribution around the Fermi level (E_F), oscillations in these properties will lead to oscillations in almost all other physical properties. Such oscillatory behavior, and other properties that originate from the standing electron waves in thin metal films, are generally referred to as quantum size effects (QSE). Consequences of the QSE have been experimentally observed, for example, as oscillations in the magnitude of electron-phonon coupling,⁴ critical temperature of superconductivity⁵ and chemical reactivity⁶ of thin films as a function of their thickness.

The formation of islands with specific "magic" heights or "critical" thicknesses preferred over others because of their lower total energy⁷ is one of the most prominent results of electron confinement in thin films.^{8-10,12-19} For example, Ag thin films deposited on Fe(100) with specific thicknesses (1, 2, and 5 monolayers) are stable due to their lower total electronic energy, whereas

films with other thicknesses rearrange into $N \pm 1$ monolayer.⁸ Impact of QSE on thin film morphology has been observed in many systems like Pb/Si(111),⁹⁻¹¹ Sn/Si(111),¹⁴ Pb/graphite,¹⁵ Ag/NiAl(110),¹⁶ Pb/Cu(111)^{17,18} and Ag/Si(001)¹⁹ to name a few. It has been also observed on several quasicrystalline systems like Ag/i-Al-Pd-Mn quasicrystal and Bi/i-Al-Pd-Mn, Al-Cu-Fe and, decagonal (d)-Al-Ni-Co quasicrystals.^{12,13,20} It has been argued that the total energy minimization due to the position of QWS with respect to E_F is responsible for the occurrence of "magic" heights in the deposited film.^{17,18}

Necessary condition for the formation of QWS is the confinement of electrons within the film thickness. The confining barrier is provided by the surface potential barrier at the vacuum-metal side and by a bandgap in the substrate electronic structure prohibiting the propagation of electronic wave function at the film-substrate interface. Consequently, electronic waves are multiply reflected from the walls of the potential well created by the vacuum/metal and metal/substrate interfaces and form the QWS.²¹⁻²³ Unlike semiconductors, there is no gap at E_F in a metal but gaps can occur along specific symmetry directions and electrons in that particular direction (usually perpendicular to the film) can be confined. Such a gap can be a "relative" gap, a hybridization gap or a symmetry gap.^{22,23}

Quasicrystals (QC's) are complex metallic alloys exhibiting anomalous properties such as high electrical resistivity, low thermal conductivity, low friction coefficient and low surface energies.^{24,25} An interesting feature of the electronic structure of many i-QC's is the formation of a "pseudogap", *i.e.* a minimum in the electronic DOS close to E_F , due to both structural and *sp-d* hybridization effects.²⁶⁻³¹ Many of the outstanding properties such as their anomalous transport properties have been attributed to the existence of the pseudogap.²⁵ High quality quasicrystalline surfaces have been prepared and their electronic structure and morphology have been studied in detail.³²⁻³⁶ This has stimulated interest in the formation of quasiperiodic metallic films, using the quasicrystalline surface as a template. Templated quasiperiodic overlayers have been achieved so far only for a few metal overlayers (Sb, Bi, Cu, Pb, Sn)³⁷⁻⁴⁴ as well as molecular layers.⁴⁵⁻⁴⁷

However, studies of metal/QC's heteroepitaxial system have revealed other interesting phenomena like heterogeneous nucleation of adatoms at specific quasilattice trap sites and the formation of nano-crystalline domains oriented along specific directions of the QC substrate.⁴⁸⁻⁵³

QC's offer much more structural and chemical complexity than elemental metals and could lead to the formation of exotic nanostructures in metal/QC systems. For example, the combination of heterogeneous nucleation and QSE at QC surfaces may result in the formation of nano islands quasiperiodically distributed on the surface and having specific heights. First indications for QSE in metal/QC systems came from STM studies of Bi and Ag thin films grown on icosahedral (*i*)-Al-Cu-Fe and *i*-Al-Pd-Mn QC's respectively.¹² The formation of islands of specific heights was achieved in both cases. A similar height selection mechanism was observed during the growth of Bi on *i*-Al-Pd-Mn, *i*-Al-Cu-Fe and decagonal *d*-Al-Ni-Co by STM.¹³ The confinement of *sp* electrons within the film was first ascribed to the pseudogap in the partial *sp* DOS of the QC substrate.¹² Evidence for QWS in metal/QC systems was reported later by Moras *et al.* in an angle resolved photoemission spectroscopy (ARPES) study of Ag overlayers on *i*-Al-Pd-Mn and *d*-Al-Ni-Co QC's. In both systems, the formation of Ag *s,p*-QWS for 7 and 14 monolayer (ML) thick Ag film could be clearly observed.²⁰ Because the total densities of states near E_F of these two QC substrates are different, it was argued that the pseudogap is not the confining barrier in these systems. Instead, it has been proposed that incompatible point group symmetries of crystalline Ag film and quasicrystalline substrates is the origin of the confinement.²⁰

The growth of Ag thin films on various QC's and specially on the *i*-Al-Pd-Mn has been studied in detail using STM and low energy electron diffraction (LEED).^{48,49,54} At room temperature and below 1 ML, flux independent nucleation of Ag adatoms on *i*-Al-Pd-Mn surface indicated heterogeneous nucleation due to the capture of adatoms at specific trap sites. Islands were mainly of mono-atomic height. At 1 ML coverage (θ), Ag films exhibited very rough three-dimensional (3D) island (up to 4-5 atoms high) growth. The large roughness of the film was related to the easy uphill motion of Ag atoms and was ascribed to thermodynamic effects (low surface energy of

substrate) rather than kinetic limitations. For $1 < \theta < 10$ ML, Ag islands grow laterally up to 30-40 nm. However, the film roughness remained approximately the same. Above 10 ML, pyramid-like nanocrystals with hexagonal flat tops develop. Film roughness also increases from about 1 nm at 10 ML up to 5 nm at 100 ML. The film consisted in five rotational domains of Ag(111) nanocrystals as evidenced by LEED patterns, thus reflecting the 5-fold rotational symmetry of the *i*-Al-Pd-Mn substrate.^{48,49} The nucleation and growth of Ag islands on the same surface was also investigated as a function of deposition temperature and flux, for $\theta < 1$ ML.⁵⁴ It was shown that films are rather smooth when deposited at or below 200 K, but become rough at 300 K or above. This indicates that the uphill migration necessary for the formation of 4-5 layer islands gets activated between 200 and 300 K.⁵⁴ It was also shown that Ag island density on *i*-Al-Pd-Mn surface is independent of deposition temperature up to 300 K, but decreases abruptly above 300 K, for a typical flux. This indicates that traps are saturated at and below 300 K, but are unsaturated at 345 K.

The *i*-Al-Cu-Fe and *i*-Al-Pd-Mn are isostructural quasicrystalline phases.^{55,56} Their surfaces perpendicular to the 5-fold axis are almost identical down to atomic scale, although their chemical compositions are of course different.⁵⁷ Similar to other icosahedral QC's, *i*-Al-Cu-Fe also exhibits a pseudogap around E_F .^{30,31,58,59} Here we report on the influence of the deposition temperature on the growth and morphology of Ag thin films on the 5-fold surface of *i*-Al-Cu-Fe as well as their electronic structure using STM, LEED, and ultraviolet photoemission spectroscopy (UPS). For the highest deposition temperature investigated in this work (400 K), we observe the formation of 3D Ag islands with specific height and the appearance of QWS in the valence band. The evolution of the QWS is studied over a wide range of Ag coverages, up to 42 ML. Possible origins of the QSE in this metal/QC system is discussed in the light of density of states calculations performed on a 2/1 approximant of the isostructural *i*-Al-Pd-Mn phases.

Experimental method and Computational details

A single grain of the *i*-Al-Cu-Fe QC phase with bulk composition $\text{Al}_{63}\text{Cu}_{24}\text{Fe}_{13}$ has been grown at the Ames Laboratory and a sample has been extracted presenting a surface oriented perpendicularly to a 5-fold axis. The surface was mechanically polished using diamond paste down to 0.25 μm . Experiments have been conducted in a UHV multi-chamber system consisting of an analysis chamber (photoemission), a preparation chamber (sample cleaning and LEED) and an STM chamber. All the chambers are interconnected through a common transfer chamber. The base pressures were $< 5 \times 10^{-11}$ in all chambers. STM experiments were performed using an Omicron variable temperature microscope. UPS experiments were carried out using an Omicron EA 125 electron energy analyzer and He I radiation ($h\nu = 21.2$ eV). The resolution of the UPS is about 90 meV at measurement temperature (300 K). A clean surface was obtained by repeated cycles of Ar^+ sputtering (1.5 keV, 30 minutes) and annealing (2 hours) up to 900 K. Surface cleanliness was checked by recording the O KLL Auger signal. This surface preparation method produces step-terrace surface morphology, with a chemical composition of the near-surface region close to the bulk composition.^{60–62} The structural quality of the *i*-Al-Cu-Fe surface was checked by STM and such surface produced a sharp 5-fold LEED pattern. Ag was evaporated using a well-degassed e-beam evaporator (EFM 3, Omicron) in the STM chamber and the pressure was kept $< 3 \times 10^{-10}$ mbar during deposition. Coverages were estimated from STM images at submonolayer coverages. As the Ag islands grow 3D on this surface, these images were thresholded to determine which fractional area of the surface covered by 1 layer high islands, 2 layers high islands, etc... in order to determine the total coverage. STM images have been recorded at deposition temperature and STM data were processed using WsXM image processing software.⁶⁴

The ground state properties of the 2/1 AIPdMn approximant are calculated by Density Functional Theory (DFT), using the plane wave Vienna ab initio simulation package (VASP).^{65–68} The interaction between the valence electrons and the ionic core is described using the projector-augmented wave (PAW) method^{69,70} within the generalized gradient approximation (GGA-PBE),^{71,72} considering the valences for the atoms to be $3s^23p^1$ (Al), $5s^14d^9$ (Pd), $3p^64s^13d^6$ (Mn). Total ener-

gies are minimized until the energy differences become less than 10^{-5} eV between two electronic cycles during the structural optimization. Atomic structures are relaxed till the Hellmann-Feynman forces are as low as 0.02 eV/Å. Total energy calculations were performed using a 400 eV cut-off energy (Ecut) and a $5 \times 5 \times 5$ k-points within the Brillouin zone.

Results and Discussion

We have investigated the growth morphology of Ag thin films on the *i*-Al-Cu-Fe surface at different coverages and deposition temperatures (57, 300 and 400 K). STM images show that the Ag film grows according to a Vollmer-Weber growth type where it reduces interfacial area by forming 3D islands. This is observed at all temperatures. For a coverage of about 1 ML, height histograms of STM images show that Ag islands are either 1, 2 or, 3 ML in height at all the deposition temperatures (Fig. 1). Island density continuously decreases with increasing deposition temperature. This observation is in agreement with the previous report of dependence of island density with deposition temperature in Ag/*i*-Al-Pd-Mn and it has been related to the unsaturated trap sites for deposition temperature ≥ 300 K.⁵⁴ This happens due to the dissociation of islands at trap sites at high temperatures before reaching their critical size.⁵⁴ The root-mean-square roughness deduced from STM images at 1 ML coverage increases with the deposition temperature and takes values similar to those reported for Ag/*i*-Al-Pd-Mn.⁷³ Height histograms show that 3 ML high islands are more frequent after deposition at 400 K compared to 57 K, indicating that easy uphill motion of Ag adatoms is facilitated at higher temperatures.^{48,49} For 1 ML Ag/*i*-Al-Pd-Mn at 365 K, it has been found that specific height (4-5 ML) flat-topped islands are preferred compared to other heights (1, 2, and 3 ML). It was suggested that uphill diffusion barrier as well as barrier associated with potential well formed by the trap sites can be overcome at deposition temperature ≥ 365 K.¹² For 1 ML Ag/*i*-Al-Cu-Fe at 400 K, we have also observed that the island tops are much flatter than for islands formed at lower temperature deposition (Fig. 2a). Due to the observation of flat-topped islands and earlier report of QSE in Ag/*i*-Al-Pd-Mn¹² at 365 K deposition temperature, we focused

our attention on the higher coverages of Ag on i-Al-Cu-Fe deposited at 400 K rather than lower deposition temperatures.

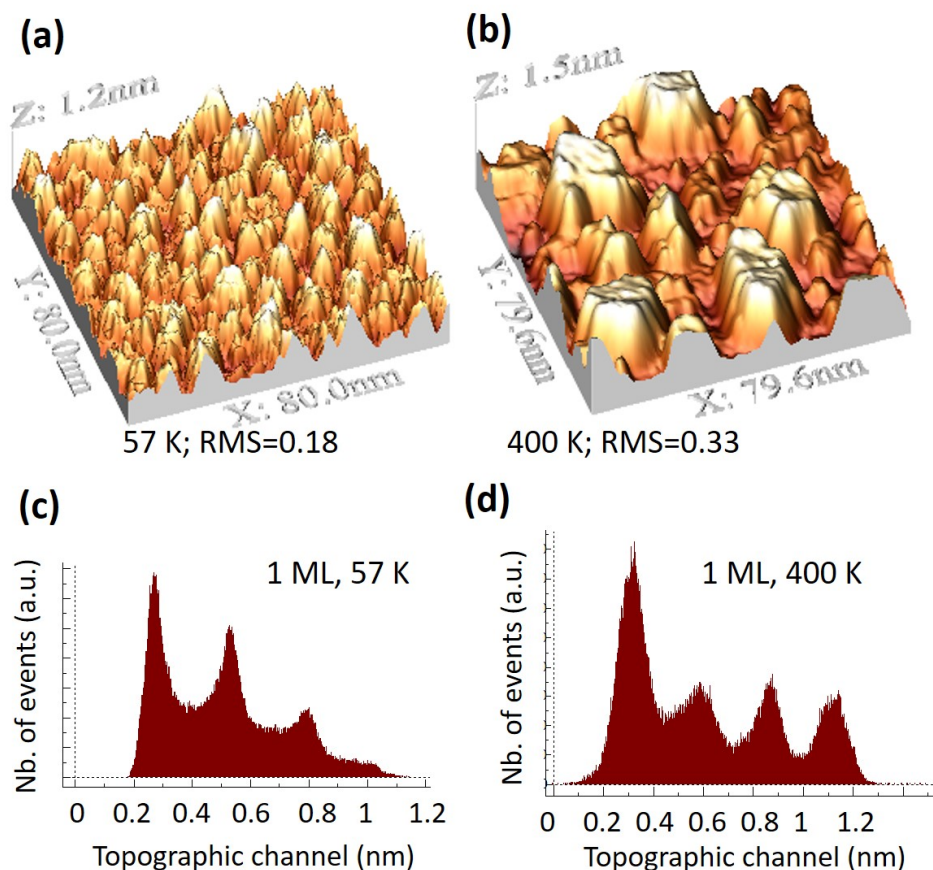


Figure 1: (a,b) STM images ($80 \times 80 \text{ nm}^2$) of the i-Al-Cu-Fe surface after dosing 1 ML Ag at 57 K and 400 K respectively and (c, d) corresponding height histograms. The root mean square roughness (RMS) values are also indicated for each temperature.

With increasing Ag coverage, lateral size and height of flat-topped islands increased. For $\theta \geq 5 \text{ ML}$, we found that there are some particular island heights more frequently observed than others. Figure 2(b) shows a STM image of 7 ML Ag dosed on 5-fold surface of i-Al-Cu-Fe at 400 K and heights of the Ag islands are indicated in Å. It is evident from Fig. 2(b) that the height of most islands is 19 Å. The Ag islands are of irregular shape with smooth tops. The average lateral size of the islands is about 50 nm. We have calculated the areas of islands of different heights from many (> 20) STM images of various sizes. Figure 2(c) shows the area covered by islands

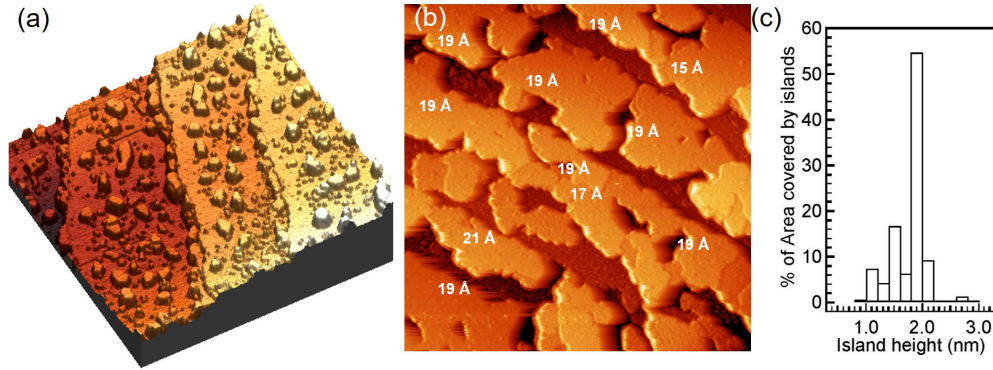


Figure 2: (a) STM image ($400 \times 400 \text{ nm}^2$) of Ag/i-Al-Cu-Fe after dosing 1 ML Ag at 400 K showing islands up to 3 ML in height. (b) STM image ($300 \times 300 \text{ nm}^2$) of Ag/i-Al-Cu-Fe after dosing 7 ML Ag at 400 K. Island heights are indicated. Tunneling conditions are -2.4 V and 0.3 nA. (c) Distribution of island heights (percentage of area covered by a given height) for 7 ML Ag on i-Al-Cu-Fe dosed at 400 K.

of different heights. It clearly shows that 19 \AA ($\approx 7 \text{ ML}$) and 15 \AA ($\approx 5 \text{ ML}$) high islands are the most preferred or "magic" height islands. The occurrence of "magic" height reveals a special stability associated with islands of specific thickness. As discussed in the introduction, formation of "magic" height islands has been observed in similar systems like Bi/i-Al-Cu-Fe and Ag/i-Al-Pd-Mn^{12,13} and for metal thin film growth on metallic and semiconductor substrates, all interpreted in terms of QSE.^{10,14,16-19} QSE can lead to the formation of QWS and consequently modify the electronic structure of films. QWS energy position depends on the film thickness and it can affect the electronic contribution to the total energy of the film.^{4,8-10,17,18} Therefore, islands or films of a specific thickness can have enhanced stability over other thicknesses due to QSE. It has been shown that the most stable islands or films are those for which QWS are placed far away from the Fermi energy.^{4,8-10,17,18} Other thicknesses for which QWS lie near E_F will have enhanced DOS at E_F and will be less stable due to the increase in electronic energy.

Crystalline order and orientation of deposited film can be monitored by LEED. Figure 3(a) shows a LEED pattern of the clean surface exhibiting 5-fold symmetry. Figures 3 (b) and (c) show LEED patterns after dosing 7 ML Ag/i-Al-Cu-Fe at 300 and 400 K respectively. Both patterns exhibit a ring centered at the surface normal and it converges towards the specular (00) spot when

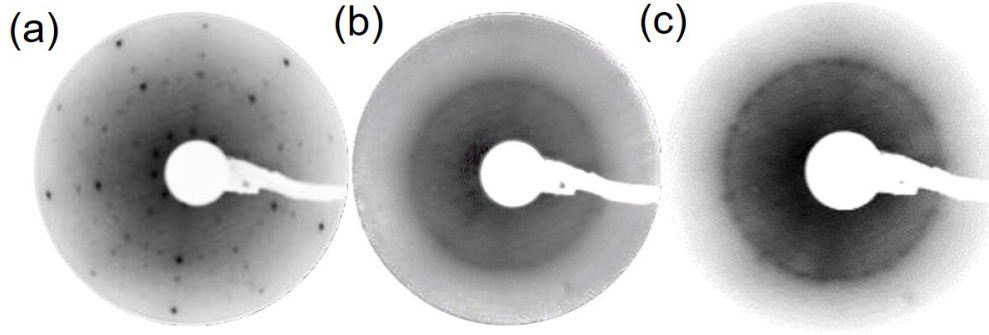


Figure 3: (a) LEED pattern of the clean surface at 60 eV primary beam energy, (b) after dosing 7 ML at 300 K and (c) after dosing 7 ML at 400 K. Incidence electron beam energy is 133 eV for both (b) and (c).

the primary electron beam energy is increased. Closer inspection reveals that the ring contains 30 spots which is more evident for the film deposited at 400 K. It indicates that crystalline order is better for films grown at 400 K compared to 300 K. Similar LEED patterns have been obtained earlier for thick layers of Ag on *i*-Al-Pd-Mn and such patterns have been related to the five different in-plane orientations of fcc Ag(111) nanocrystals with their [111] axis parallel to the one of 5-fold axis of the *i*-Al-Pd-Mn substrate.^{20,49} Therefore, the LEED patterns for thick coverages indicate that Ag grows as 5-fold twinned (111)-oriented nanocrystals, similar to the case of Ag/*i*-Al-Pd-Mn.

QSE effects in thin metal films are generally manifested in form of QWS as observed by photoemission spectroscopy.^{22,23} Information on the electronic structure of the substrate is necessary to understand the origin and energy positions of QWS. In Figure 4(a), we show the UPS valence band (VB) spectrum of the clean *i*-Al-Cu-Fe substrate. Two peaks are visible in the spectrum. The peak at 1 eV binding energy (BE) is due to the Fe 3d like band and the peak at 4.2 eV is related to the Cu 3d like band.^{30,31,58,59} The VB spectrum exhibits the rounding of E_F due to the reduction of the DOS towards E_F and it is usually interpreted as the signature of the pseudogap close to E_F .⁶³ Our VB spectrum is in good agreement with earlier published spectra of the clean *i*-Al-Cu-Fe.^{31,58,59} Figure 4 (b) shows the normal emission UPS VB spectra as a function of Ag film thickness deposited on the *i*-Al-Cu-Fe surface at 400 K. For $\theta \geq 3$ ML, a peak appears near to E_F . Its intensity increases and energy position shifts towards E_F with increasing Ag coverage and finally settles just below E_F for $\theta \geq 14$ ML. The VB spectrum of 42 ML thick Ag film is almost

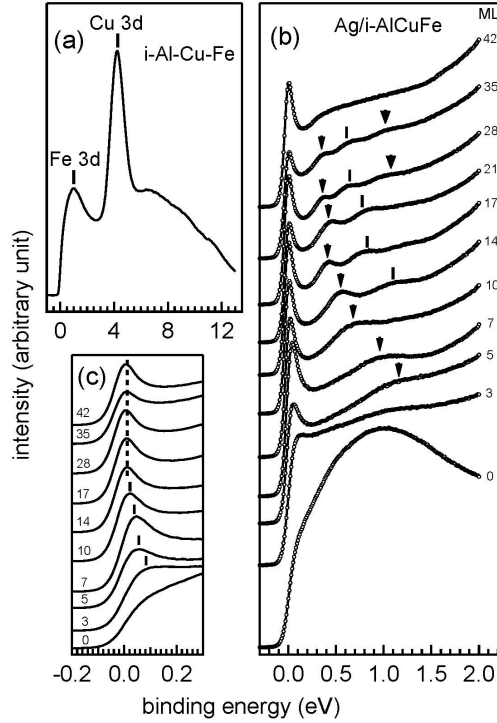


Figure 4: (a) UPS valence band spectrum of clean i-Al-Cu-Fe, (b) UPS valence band spectra for the Ag films of varying thickness on i-Al-Cu-Fe surface deposited at 400 K. Coverages are indicated in units of monolayers at the right hand side. Peak positions of first quantum well state are indicated by thin arrows, second quantum well state by ticks and of third quantum well state by thick arrows. (c) Near Fermi edge region of a few spectra shown in Fig. 1(b). All the UPS spectra have been collected in the normal emission geometry at the room temperature. Occupied states are referred to positive energies with respect to the Fermi level in these graphs.

similar to previously reported spectra for Ag(111) thick films^{74–78} and for bulk Ag(111) clean surface.^{79–81} From the comparison of these earlier reports, intense and sharp feature just below the E_F is assigned to the Ag(111)-derived Shockley type surface state (SS) confined in the L gap. Near E_F spectra (Fig. 4(c)) highlights the BE variation (indicated by ticks and dashed line) of SS at lower coverages of Ag. It has been shown earlier that the BE of Ag(111) related SS changes with the film thickness due to the finite decay length of SS wave function.^{75,77,80,82,83} Decay length of SS depends on the electronic structure of the substrate and it ranges from 6 to 12 ML.^{75,77,80,82,83} Above its decay length, the BE of Ag(111) SS remains nearly the same as its bulk value decay length.^{75,83} Comparison of SS BE position in our case with earlier reports indicates that decay length of SS in Ag/i-Al-Cu-Fe is between 10 to 14 ML. Intense SS (Fig. 4(b)) above 7 ML shows

the good crystallinity and orientation of Ag islands.

Figure 4(b) also shows the evolution of additional fine structures (indicated by thin and thick arrows and ticks) at higher BE side of SS with increasing Ag coverage. These features are not observed in Ag(111) single crystal.⁸¹ The BE of these spectral features shifts towards lower BE and energy interval decreases between them with increasing film thickness. Ag(111) film growth on various substrates has shown similar spectral features in VB spectra and these have been interpreted as the Ag sp QWS.^{18–20,22,23,84} Therefore, features observed in the VB spectra of Ag/i-Al-Cu-Fe between 0.35 and 1.2 eV are the QWS due to the confinement of Ag sp electrons in the potential well along the normal to the film formed by vacuum/Ag and Ag/i-Al-Cu-Fe interfaces. The first QWS is observed at 1.16 eV for 5 ML film and its BE decreases continuously with increasing film thickness and reaches 0.35 eV for 35 ML coverage as indicated by thin arrows in Fig. 4(b). The second QWS is observed at 14 ML (indicated by ticks) and the third QWS (indicated by thick arrows) appears at 28 ML. The BE of QWS shifts towards lower values at higher coverage due to the increase of the width of the confining potential well.^{22,23} Λ_6 sp band of Ag(111) exhibits the gap at 0.3 eV at the L edge and therefore all the QWS are trapped at this band edge and can never cross the E_F .^{22,23} This is nicely exhibited by our VB spectra (Fig. 4(b)) as the highest occupied QWS is situated at 0.35 eV for 35 ML.

Figure 5 shows the VB UPS spectra of 7 ML Ag/i-Al-Cu-Fe deposited at 300 and 400 K substrate temperatures. Comparison of the two spectra clearly shows that the QWS (indicated by tick) and Ag(111)-derived SS are quite broad and weak for 300 K deposition. Sharper SS at 400 K suggests that the crystallinity of the film deposited at 400 K is better than the film deposited at 300 K, in agreement with the LEED observation (Fig. 3). The broadening of QWS observed for 300 K deposition suggests that the height distribution of islands is probably larger compared to that of the film grown at 400 K. According to the previously discussed STM data, the film thickness is not completely homogeneous even after depositing the film at 400 K, but the height distribution is sufficiently narrow such that QWS emerge in the photoemission spectra. An attempt to form the film at low temperature (57K) followed by room temperature annealing as suggested by Moras *et*

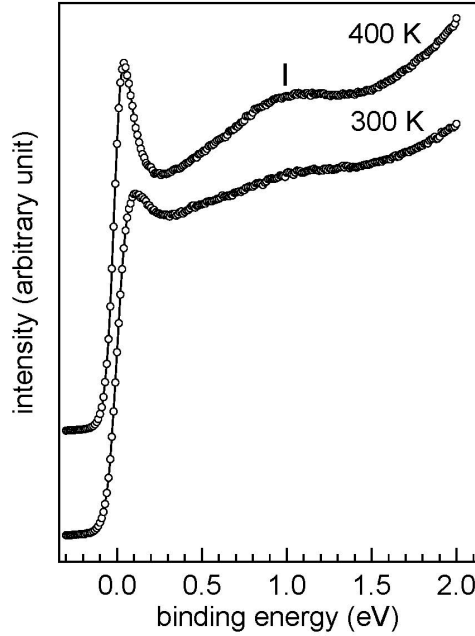


Figure 5: Normal emission UPS valence band spectra of 7 ML Ag film deposited on i-Al-Cu-Fe at 300 and 400 K. Spectra were collected at room temperature. Position of the quantum well state is indicated by tick.

*al.*²⁰ did not allow to improve the thickness homogeneity of the film in our case.

The origin of the confining barrier at the metal/QC interface has been interpreted based on two different scenarios.^{12,20} It was first suggested that the pseudogap in the QC DOS near E_F could provide the confining barrier for Ag and Bi sp electrons at Ag/i-Al-Pd-Mn and Bi/i-Al-Cu-Fe interfaces.¹² Later, Moras *et al.* argued that the pseudogap can not act as the confining barrier as it is typically narrow (on the order of 0.5 eV) and Ag sp QWS are observed well above this gap (up to 1.16 eV in our case for Ag/i-Al-Cu-Fe and up to ≈ 2.4 eV for Ag/d-Al-Ni-Co).²⁰

As mentioned previously, the formation of QWS requires an energy gap in the substrate electronic structure and it may not be strictly a true bandgap. Mismatch in the symmetry character of overlayer and substrate electrons can create such a gap as it has been shown for systems like Ag/Fe(100), Ni(111), and V(100).^{22,84-87} For example, it has been reported that the sp symmetry of the V(100) substrate DOS near E_F acts as an efficient confining barrier for d-electrons of Ag overlayer.⁸⁷ Also sp as well as d-QWS have been observed in Ag/Ni(111).^{84,86} Projection of the

VB states of Ni(111) at the surface Brillouin zone shows that Ni bands of d-symmetry dominate the energy range between the Fermi energy and 2.6 eV BE and for higher BE - up to 9 eV - only sp symmetry electronic states exist.⁸⁴ Ag sp QWS in Ag/Ni(111) have been observed between ≈ 0.8 to 3.5 eV BE.⁸⁴ Ag sp QWS are confined at Ag/Ni(111) interface in the projected band gap (2.6-4.8 eV) and above this gap sp QWS are localized due to the presence of only d-symmetry electronic states in Ni(111).^{84,86} It has been shown that the s-d hybridization gap in Fe(100) defined by the d-band width acts as the confining barrier for Ag sp QWS in Ag/Fe(100).^{22,85}

According to the above literature, electron confinement of Ag sp states on i-Al-Cu-Fe could occur in principle if a gap exists in the partial sp DOS of the substrate. We have seen that the photoemission spectra of i-Al-Cu-Fe are dominated by Fe related d-states in the energy region where QWS are observed (between E_F and ≈ 2 eV, see Fig. 4(a)) but it is not possible to conclude about the absence of sp states in the valence band from such experiment, as the spectral weight of sp states is much lower than that of d states due to photoionization cross-section differences.

Therefore we have performed electronic structure calculations to shed light on the QC electron density in the vicinity of E_F . The calculations are performed for approximant structures, i.e. periodic crystals having a local structure and a chemical composition that are very similar to those of the quasicrystal. As well accepted structural models for approximants of the i-Al-Cu-Fe phase are lacking, calculations were performed for the isostructural i-Al-Pd-Mn system for which a so-called 2/1 approximant has been constructed using the cut-and-projection technique in the six-dimensional hyperspace according to the Katz-Gratias-Boudard model⁸⁸⁻⁹⁰. The 2/1 approximant consists of 544 atoms in a cubic cell (396 Al atoms, 100 Pd atoms, 48 Mn atoms) with the lattice constant $a = 20.31 \text{ \AA}$ and the $P2_13$ space-group symmetry. The calculated partial DOS are shown in Fig. 6. The pseudogap in the total DOS is clearly visible and is about 0.13 eV wide and is centered at -0.5 eV above the Fermi level. The DOS in the region of interest between E_F and ≈ 2 eV is clearly dominated by Mn d states hybridized with Al sp states. The Pd states have a negligible contribution in this energy range. Previous works have shown that the electronic structure in the Al-Cu-Fe and Al-Pd-Mn share similar features.³¹ Therefore, it is expected that both Al sp and Fe d

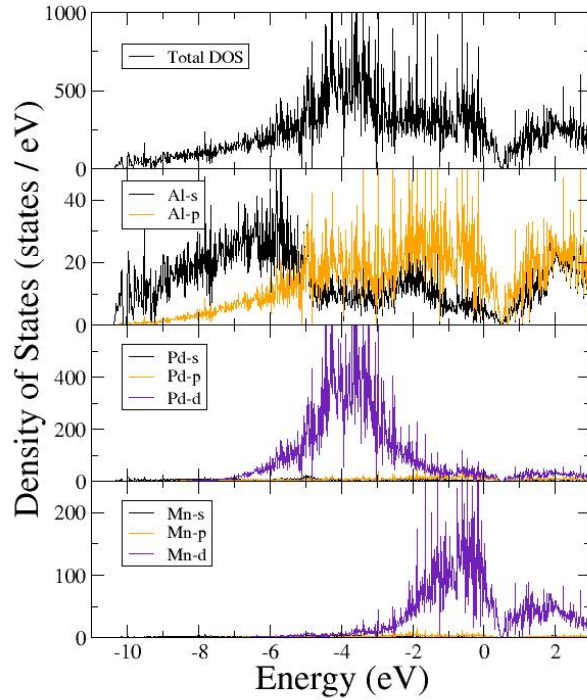


Figure 6: Calculated total and partial DOS for the 2/1 Al-Pd-Mn approximant. Occupied states are referred to negative energies with respect to the Fermi level in this graph.

states will also contribute to the substrate DOS in a similar proportion in that energy range. Therefore the confinement of Ag sp QWS at the overlayer/quasicrystal interface is probably not due to the pseudogap in the total or even partial substrate DOS. Instead, as proposed by Moras *et al.*,²⁰ it is more likely due to the lack of common point group symmetries between the metal and substrate wave functions. This conclusion is also in line with the observation that QWS appear in the photoemission spectra only if the degree of crystallinity of the Ag film is high enough, here facilitated by high temperature deposition conditions as shown by the LEED patterns. Indeed, the argument of incompatible point group symmetry can only hold if the Ag film is indeed *fcc*. This may not be true at very low coverage, as the structure of at least the first Ag layer may certainly be influenced by the substrate surface, as evidenced by the report of pseudomorphic islands in Ag/i-Al-Pd-Mn at 365 K for example.⁹¹ It is likely that the structure of the Ag film evolves progressively with

increasing coverage and only recovers a well ordered *fcc* structure after a few ML. This would be in agreement with the fact that the first QWS are observed for 5 ML. It follows that QSE should be a general phenomenon in metal thin films on QC substrates.

Conclusions

In conclusion, we have studied the growth and electronic structure of Ag thin films deposited at various temperature on the 5-fold surface of the icosahedral (*i*)-Al-Cu-Fe quasicrystal using scanning tunneling microscopy (STM), low energy electron diffraction (LEED), and ultra-violet photoemission spectroscopy (UPS). Upon deposition at 400 K, Ag islands grow with a more uniform thickness and form crystallites with a better defined long-range *fcc* order compared to low deposition temperature. LEED patterns reveal five rotational domains of Ag crystallites with (111) orientation for coverages larger than ~ 7 monolayers. Quantum well states (QWS) are observed in the photoemission spectra of Ag/*i*-Al-Cu-Fe ranging from 5 to 35 monolayers, indicating electron confinement within the film thickness and thus confirming electronic growth of Ag thin films on quasicrystalline surfaces. Electronic structure calculations have been performed to discuss the possible origins of the confinement at the film-substrate interface and points toward the argument of incompatible point group symmetry between the crystalline thin film and the quasicrystalline substrate as the confinement barrier rather than a pseudogap induced confinement. It follows that QSE should be a general phenomenon in metal thin films on quasicrystalline substrates.

Acknowledgments

This work was also supported by the European C-MAC consortium and the French PIA project “Lorraine Université d’Excellence”, reference ANR-15-IDEX-04-LUE. High performance computing resources were provided by GENCI under Allocation 99642, as well as the EXPLOR center hosted by the Université de Lorraine (Allocation 2017M4XXX0108). EG acknowledges financial support through the COMETE project (COncption in silico de Matériaux pour l’Environnement

et l'Energie) funded by the Lorraine Region.

Data availability statement

The data that support the findings of this study are available from the corresponding author upon reasonable request.

References

- (1) P. J. Feibelman, Phys. Rev. B **27**, 1991 (1983).
- (2) P. J. Feibelman and D. R. Hanman, Phys. Rev. B **29**, 6463 (1986).
- (3) F. C. Schulte, Surf. Sci. **55**, 427 (1976).
- (4) Y.-F. Zhang, Jin-Feng Jia, Tie-Zhu Han, Zhe Tang, Quan-Tong Shen, Yang Guo, Z. Q. Qiu, and Qi-Kun Xue, Phys. Rev. Lett. **95**, 096802 (2005).
- (5) Y. Guo, Y.-F. Zhang, X.-y. Bao, T.-Z. Han, Z. Tang, L.-X. Zhang, W.-G. zhu, E. G. Wang, Q. Niu, J.-f. Jia, Z.-X. Zhao, and Q.-K. Xue, Science **306**, 1915 (2004).
- (6) L. Aballe, A. Barinov, A. Locatelli, S. Heun, and M. Kiskinova, Phys. Rev. Lett. **93**, 196103 (2004).
- (7) Z. Zhang, Q. Niu, and C.-K. Shih, Phys. Rev. Lett. **80**, 5381 (1998).
- (8) D.-A. Luh, T. Miller, J. J. Paggel, M. Y. Chou, and T.-C. Chiang, Science **292**, 1131 (2001).
- (9) M. H. Upton, C. M. Wei, M. Y. Chou, T. Miller, and T.-C. Chiang, Phys. Rev. Lett. **93**, 026802 (2004).
- (10) V. Yeh, L. Berbil-Baustita, C. Z. Wang, K. M. ho, and M. C. Tringides, Phys. Rev. Lett. **85**, 5158 (2000).

- (11) M. Hupalo and M. C. Tringides, *Phys. Rev. B* **65**, 115406 (2002).
- (12) V. Fournée, H. R. Sharma, M. Shimoda, A. P. Tsai, B. Unal, A. R. Ross, T. A. Lograsso, and P. A. Thiel, *Phys. Rev. Lett.* **95**, 155504 (2005).
- (13) H. R. Sharma, V. Fournée, M. Shimoda, A. R. Ross, T. A. Lograsso, P. Gille, and A. P. Tsai, *Phys. Rev. B* **78**, 155416 (2008).
- (14) L. L. Wang, X. C. Ma, S. H. Ji, Y. S. Fu, Q. T. Shen, J. F. Jia, K. F. Kelly, and Q. K. Xue, *Phys. Rev. B* **77**, 205410 (2008).
- (15) Y. Liu, J. J. Paggel, M. H. Upton, T. Miller, and T.-C. Chiang, *Phys. Rev. B* **78**, 235437 (2008).
- (16) Baris Unal, Feli Qin, Yong Han, Da-Jiang Liu, Dapeng Jing, A. R. Layson, Cynthia J. Jenks, J. W. Evans, and P. A. Thiel, *Phys. Rev. B* **76**, 195410 (2007).
- (17) Roberto Otera, Amadeo L. Vazquez de Parga, and Rodolfo Miranda, *Phys. Rev. B* **66**, 115401 (2002).
- (18) J. H. Dil, T. U. Kampen, B. Hulsen, T. Seyller, and K. Horn, *Phys. Rev. B* **75**, 161401 (2007).
- (19) Iwao Matsuda, Han Woong Yeom, Takehiro Tanikawa, Kensuke Tono, Tadaaki Nagao, Shuji Hasegawa, and Toshiaki Ohta, *Phys. Rev. B* **63**, 125325 (2007).
- (20) P. Moras, Y. Weisskopf, J.-N. Longchamp, M. Erbudak, P. H. Zhou, L. Ferrari, and C. Carbone, *Phys. Rev. B* **74**, 121405 (2006).
- (21) N. V. Smith, *Phys. Rev. B* **32**, 3549 (1985).
- (22) T.-C. Chiang, *Surf. Sci. Rep.* **39**, 181 (2000).
- (23) M. Milun, P. Pervan, and D. P. Woodruff, *Rep. Prog. Phys.* **65**, 99 (2002).
- (24) D. Shechtman, I. Blech, D. Gratias, and J. W. Cahn, *Phys. Rev. Lett.* **53**, 1951 (1984).

- (25) *Physical properties of quasicrystals*, ed. by Z. M. Stadnik, Solid State Sciences, vol. 126 (Springer, Berlin 1999).
- (26) G. T. de Laissardiere, D. N. Manh and D. Mayou, *Prog. Mater. Sci.* **50**, 679 (2005).
- (27) X. Wu , S. W. Kycia , C. G. Olson, P. J. Benning , A. I. Goldman, and D. W. Lynch, *Phys. Rev. Lett.* **75** 4540 (1995).
- (28) G. Neuhold, S. R. Barman, K. Horn, W. Theis, P. Ebert, and K. Urban, *Phys. Rev. B* **58**, 734 (1998).
- (29) D. Naumović, P. Aebi, L. Schlapbach, C. Beeli, T. A. Lograsso and D. W. Delaney, *Phys. Rev. B* **60**, R16330 (1999).
- (30) Z. M. Stadnik, D. Purdie, M. Garnier, Y. Baer, A.-P. Tsai, A. Inoue, K. Edagawa and S. Takeuchi, *Phys. Rev. Lett.* **77**, 1777 (1996).
- (31) Z. M. Stadnik, D. Purdie, M. Garnier, Y. Baer, A.-P. Tsai, A. Inoue, K. Edagawa, S. Takeuchi, and K. H. J. Buschow, *Phys. Rev. B* **55**, 10938 (1997).
- (32) M. Gierer, M. A. Van Hove, A. I. Goldman, Z. Shen, S.-L. Chang, C. J. Jenks, C.-M. Zhang, and P. A. Thiel, *Phys. Rev. Lett.* **78**, 467 (1997).
- (33) E. Rotenberg, W. Theis, K. Horn and P. Gille, *Nature* **406**, 602 (2000).
- (34) J. Zheng, C. H. A. Huan, A. T. S. Wee, M. A. Van Hove, C. S. Fadley, F. J. Shi, E. Rotenberg, S. R. Barman, J. J. Paggel, K. Horn, Ph. Ebert, and K. Urban, *Phys Rev. B* **69**, 134107 (2004).
- (35) M. Krajčí and J. Hafner, *Phys. Rev. B* **71**, 184207 (2005).
- (36) H. R. Sharma, M. Shimoda, and A. P. Tsai, *Adv. Phys.* **56**, 403 (2007).
- (37) K. J. Franke, H. R. Sharma, W. Theis, P. Gille, Ph. Ebert, and K. H. Rieder, *Phys. Rev. Lett.* **89**, 156104 (2002).

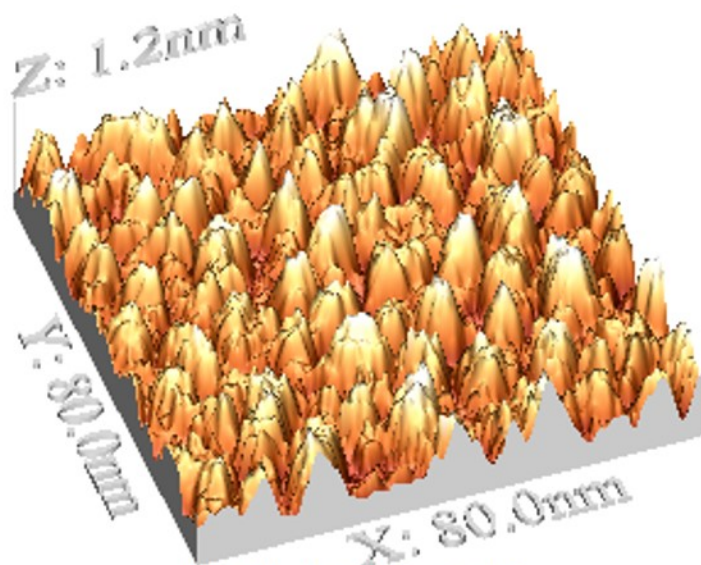
- (38) J. Ledieu, J. T. Hoelt, D. E. Reid, J. A. Smerdon, R. D. Diehl, T. A. Lograsso, A. R. Ross, and R. McGrath, *Phys. Rev. Lett.* **92**, 135507 (2004).
- (39) H. R. Sharma, M. Shimoda, A. R. Ross, T. A. Lograsso, and A. P. Tsai, *Phys. Rev. B* **72**, 45428 (2005).
- (40) J. Ledieu, L. Leung, L. H. Wearing, R. McGrath, T. A. Lograsso, D. Wu, and V. Fournée, *Phys. Rev. B* **77**, 073409 (2008).
- (41) J. A. Smerdon, J. K. Parle, L. H. Wearing, T. A. Lograsso, A. R. Ross, and R. McGrath, *Phys. Rev. B* **78**, 075407 (2008).
- (42) H. R. Sharma, K. Nozawa, J. A. Smerdon, P. J. Nugent, I. McLeod, V. R. Dhanak, M. Shimoda, Y. Ishii, A. P. Tsai and R. McGrath, *Nature Comm.* **4**, 2715 (2013).
- (43) H. R. Sharma, J. A. Smerdon, P. J. Nugent, A. Ribeiro, I. McLeod, V. R. Dhanak, M. Shimoda, A. P. Tsai, and R. McGrath, *J. Chem. Phys.* **140**, 174710 (2014).
- (44) S. Coates, S. Thorn, R. McGrath, H. R. Sharma, and A.-P. Tsai, *Phys. Rev. Materials* **4**, 026003 (2020).
- (45) V. Fournée, E. Gaudry, J. Ledieu, M. C. de Weerd, D. Wu, T. Lograsso, *ACS Nano* **8**, 3646 (2014).
- (46) J. Smerdon, K. M. Young, M. Lowe, S. S. Hars, T. P. Yadav, D. Hesp, V. R. Dhanak, A. P. Tsai, H. R. Sharma, and R. McGrath, *Nano Letters* **14**, 1184 (2014).
- (47) N. Kalashnyk, J. Ledieu, É. Gaudry, C. Cui, A-P. Tsai and V. Fournée, *Nano Research* **11**, 2129 (2018).
- (48) V. Fournée, T. C. Cai, A. R. Ross, T. A. Lograsso, J. W. Evans, and P. A. Thiel, *Phys. Rev. B* **67**, 033406 (2003).
- (49) V. Fournée, A. R. Ross, T. A. Lograsso, J. W. Evans, and P. A. Thiel, *Surf. Sci.* **537**, 5 (2003).

- (50) T. Fluckiger, Y. Weisskopf, M. Erbudak, R. Luscher, and A. R. Kortan, *Nano Lett.* **3**, 1717 (2003).
- (51) B. Bolliger, V. E. Dmitrienko, M. Erbudak, R. Luscher, H.-U. Nissen, and A. R. Kortan, *Phys. Rev. B* **63**, 052203 (2001).
- (52) Y. Weisskopf, R. Luscher, and M. Erbudak, *Surf. Sci.* **578**, 35 (2005); Y. Weisskopf, M. Erbudak, J.-N. Longchamp, and T. Michlmayr, *Surf. Sci.* **600**, 2592 (2006).
- (53) Y. Weisskopf, S. Burkardt, M. Erbudak, and J.-N. Longchamp, *Surf. Sci.* **601**, 544 (2007).
- (54) B. Unal, V. Fournée, K. J. Schnitzenbaumer, C. Ghosh, C. J. Jenks, A. R. Ross, T. A. Lograsso, J. W. Evans, and P. A. Thiel, *Phys. Rev. B* **75**, 064205 (2007).
- (55) D. Gratias, F. Puyraimond, and M. Quiquandon, *Phys. Rev. B* **63**, 024202 (2000).
- (56) A. Yamamoto, *Phys. Rev. Lett.* **93**, 195505 (2004).
- (57) H. R. Sharma, M. Shimoda, and A. P. Tsai, *Jpn. J. Appl. Phys., Part I* **45**, 2208 (2006).
- (58) G. T. de Laissardière, and T. Fujiwara, *Phys. Rev. B* **50**, 5999 (1994).
- (59) J. A. Barrow, V. Fournée, A. R. Ross, P. A. Thiel, M. Shimoda, and A. P. Tsai, *Surf. Sci.* **539**, 54 (2003).
- (60) T. Cai, V. Fournée, T. Lograsso, A. Ross, and P. A. Thiel, *Phys. Rev. B* **65**, 140202 (2002).
- (61) H. R. Sharma, V. Fournée, M. Shimoda, A. R. Ross, T. A. Lograsso, A. P. Tsai, and A. Yamamoto, *Phys. Rev. Lett.* **93**, 165502 (2005).
- (62) Th. Deniozou, J. Ledieu, V. Fournée, D. M. Wu, T. A. Lograsso, H. I. Li, and R. D. Diehl, *Phys. Rev. B* **79**, 245405 (2009).
- (63) J. Nayak, M. Maniraj, A. Rai, S. Singh, P. Rajput, A. Gloskovskii, J. Zegenhagen, D. L. Schlagel, T. A. Lograsso, K. Horn, and S. R. Barman, *Phys. Rev. Lett.* **109**, 216403 (2012).

- (64) I. Horcas, R. Fernández, J.M. Gómez-Rodríguez, J. Colchero, J. Gómez-Herrero and A.M. Baró. *Review of Scientific Instruments* **78**, 013705 (2007)
- (65) G. Kresse and J. Hafner, *Phys. Rev. B* **47**, 558 (1993).
- (66) G. Kresse and J. Hafner, *Phys. Rev. B* **49**, 14251 (1994).
- (67) G. Kresse and J. Furthmüller, *Phys. Rev. B* **54**, 11169 (1996).
- (68) G. Kresse and J. Furthmüller, *Comput. Mater. Sci.* **6**, 15 (1996).
- (69) P. E. Blochl, *Phys. Rev. B* **50**, 17953 (1994).
- (70) G. Kresse and D. Joubert, *Phys. Rev. B* **59**, 1758 (1999).
- (71) J. P. Perdew, K. Burke, and M. Ernzerhof, *Phys. Rev. Lett.* **77**, 3865 (1996).
- (72) J. P. Perdew, K. Burke, and M. Ernzerhof, *Phys. Rev. Lett.* **78**, 1396 (1997).
- (73) B. Unal, J. W. Evans, and P. A. Thiel, *Acta Physica Polonica A* **126**, 608 (2014).
- (74) T. Miller, A. Samsaver, G. E. Franklin, and T.-C. Chiang, *Phys. Rev. Lett.* **61**, 1404 (1988).
- (75) A. L. Wachs, A. P. Shapiro, T. C. Hsieh, and T.-C. Chiang, *Phys. Rev. B* **31**, 1460 (1986).
- (76) M. A. Mueller, T. Miller, and T.-C. Chiang, *Phys. Rev. B* **41**, 5214 (1990).
- (77) F. Patthey and W.-D. Schneider, *Surf. Sci.* **334**, L715 (1995).
- (78) K. Takahashi, A. Tanaka, M. Hatano, K. Tamura, S. Suzuki, and S. Sato, *J. Electron Spectrosc. Relat. Phenom.* **88**, 347 (1998).
- (79) P. Heimann, H. Neddermeyer, and H. F. Roloff, *J. Phys. C* **10**, L17 (1977).
- (80) A. P. Shapiro, A. L. Wachs, and T.-C. Chiang, *Solid State Commun.* **58**, 121 (1996).
- (81) S. D. Kevan and R. H. Gaylord, *Phys. Rev. B* **36**, 5809 (1987).

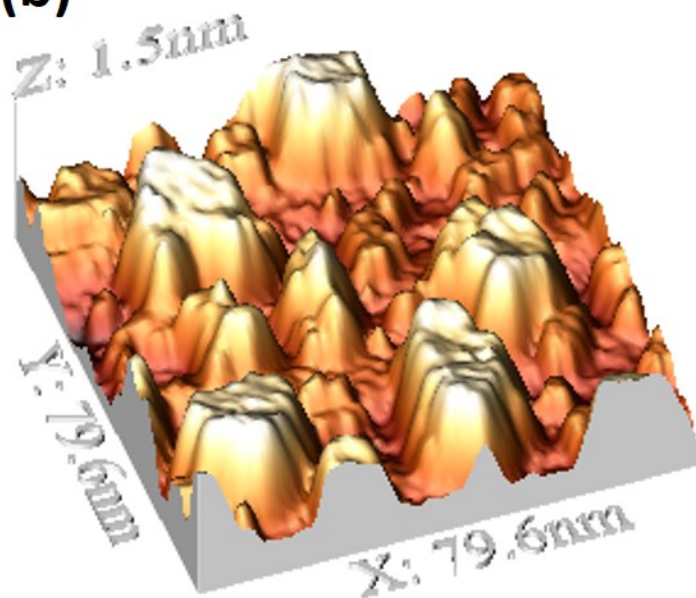
- (82) T. C. Hsieh, T. Miller, and T. -C. Chiang, Phys. Rev. Lett. **55**, 2483 (1985).
- (83) Li Huang, X. G. Gong, E. Gergert, F. Forster, A. Bendounan, F. Reinert, and Z. Zhang, Europ. Phys. Lett. **78**, 57003 (2007).
- (84) A. Varykhalov, A. M. Shikin, W. Gudat, P. Moras, C. Grazioli, C. Carbone, and O. Rader, Phys. Rev. Lett. **95**, 247601 (2005).
- (85) N. V. Smith, N. B. Brookes, Y. Chang, and P. D. Johnson, Phys. Rev. B **49**, 332 (1994).
- (86) V. Miksic Trontl, P. Pervan, and M. Milun, Surf. Sci. **603**, 125 (2009).
- (87) M. Kralj, P. Pervan, M. Milun, T. Valla, P. D. Johnson, and D. P. Woodruff, Phys. Rev. B **68**, 245413 (2003).
- (88) M. Krajci, M. Windisch, J. Hafner, G. Kresse, and M. Mihalkovič, Phys. Rev. B **51**, 17355 (1995).
- (89) A. Katz and D. Gratias, J. Non Cryst. Solids **153-154**, 187 (1993).
- (90) M. Boudard, M. de Boissieu, C. Janot, G. Heger, C. Beeli, H.-U. Nissen, H. Vincent, R. Ibberson, M. Audier, and J. M. Dubois, J. Phys. Condens. Matt. **4**, 10149 (1992).
- (91) B. Unal, V. Fournée, P. A. Thiel, and J. W. Evans, Phys. Rev. Lett. **102**, 196103 (2009).

(a)



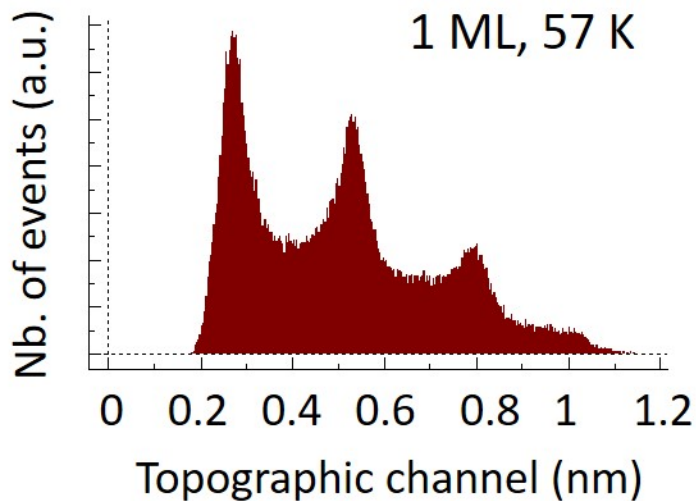
57 K; RMS=0.18

(b)

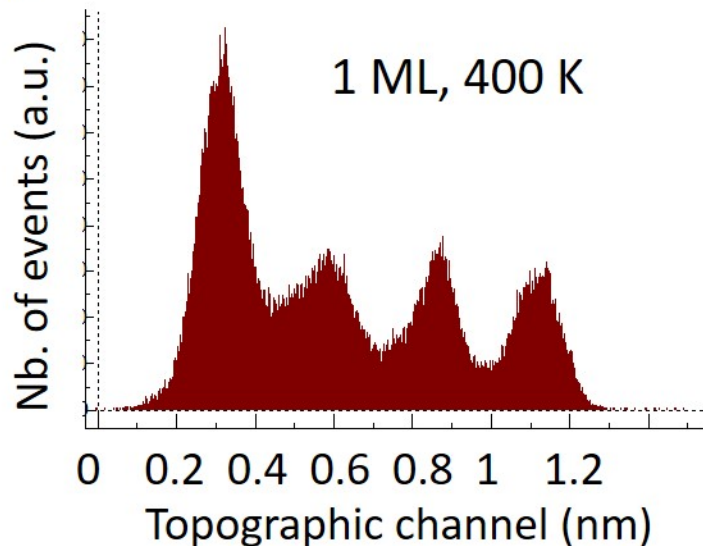


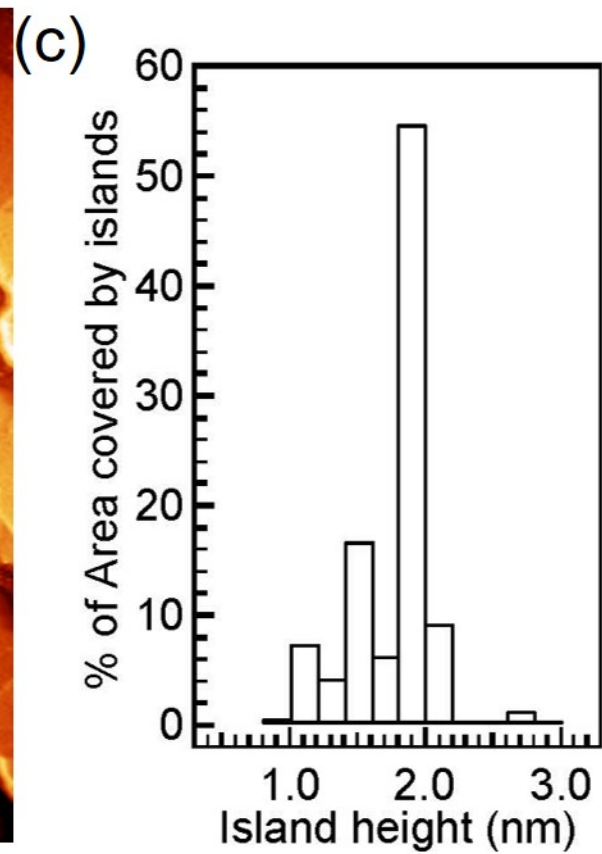
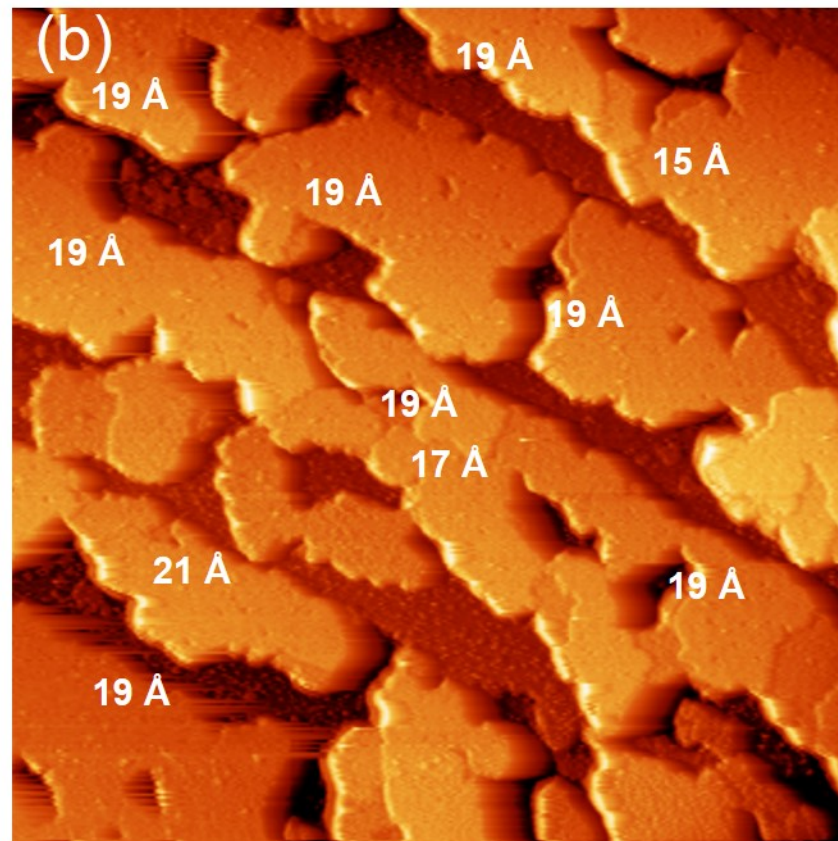
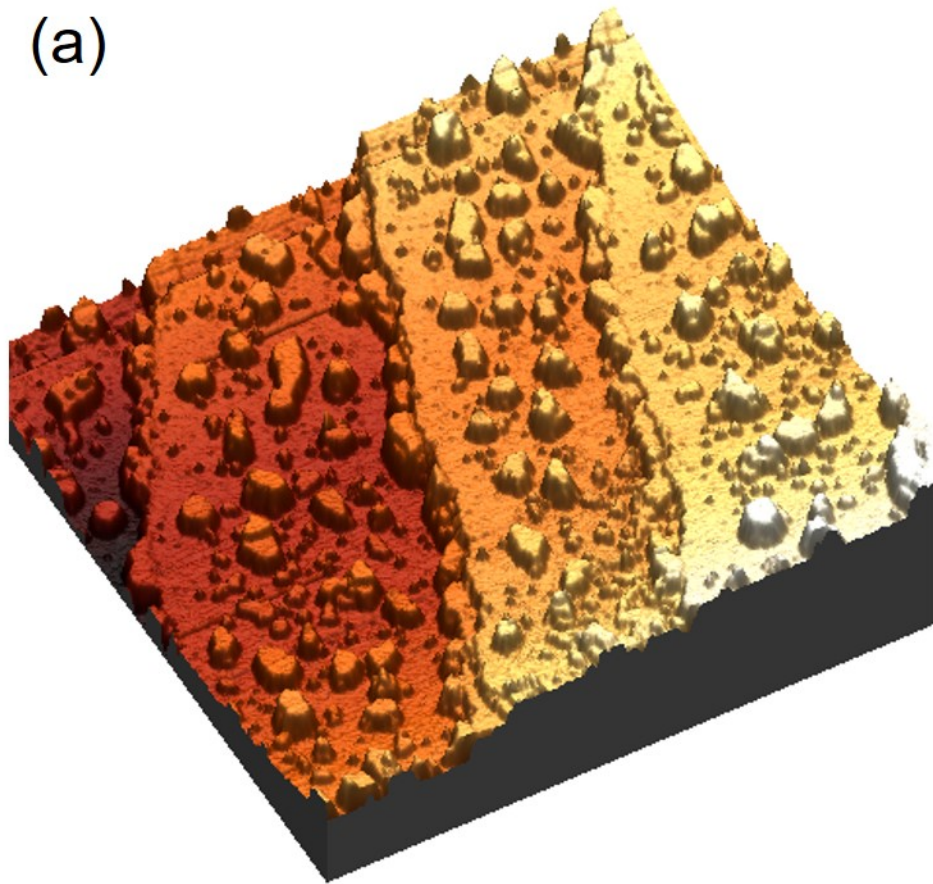
400 K; RMS=0.33

(c)

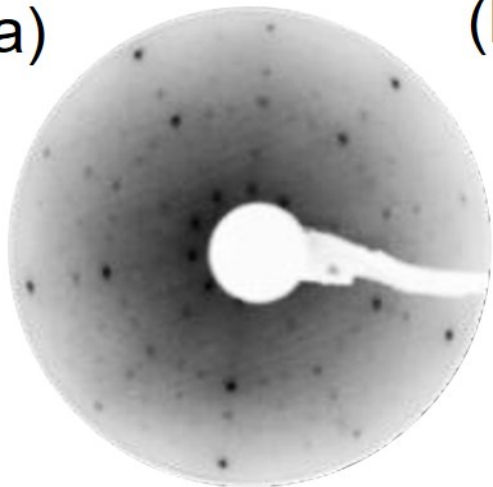


(d)

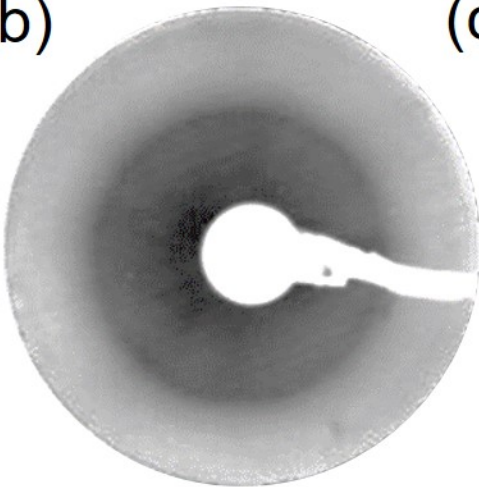




(a)



(b)



(c)

